IJPSR (2026), Volume 17, Issue 5 (Research Article)

INTERNATIONAL JOURNAL OF PHARMACEUTICAL SCIENCES AND RESEARCH

Received on 24 December 2025; received in revised form, 05 January 2026; accepted, 14 January 2026; published 01 May 2026

DESIGNING EFFICIENT SOLID LIPID NANOPARTICLES FOR COLORECTAL CANCER: FORMULATION AND EVALUATION OF ESCULIN AND SILYMARIN USING DoE APPROACH

Kiran Birje [*1] and Omkar Shelar [2]

Department of Pharmaceutical Quality Assurance [1], Department of Pharmaceutics [2], KLE College of Pharmacy, Belagavi - 590010, Karnataka, India.

Keywords:

Colorectal cancer, Solid lipid nanoparticles, Silymarin, Esculin, Design of experiment

Correspondence to Author:
Kiran Birje

Research Scholar,
Department of Pharmaceutical Quality Assurance, KLE College of Pharmacy, Belagavi - 590010, Karnataka, India.

E-mail: kiranbirje137@gmail.com

ABSTRACT: This research focused on formulating and optimizing solid lipid nanoparticles (SLNs) loaded with esculin and silymarin to enhance their physicochemical stability and *in-vitro* anticancer activity against colorectal cancer cells. The SLNs were produced using a hot homogenization method, and a 3^2 factorial design in Design Expert® software was employed to assess the effect of glyceryl monostearate (GMS) and Tween-80 concentrations on particle size (PS), zeta potential (ZP), and entrapment efficiency (EE). The optimized batch containing 1% (w/w) GMS and 2% (w/w) Tween-80 achieved a PS of 152 nm, ZP of −27 mV, and EE of 84.6%. Transmission electron microscopy revealed spherical particles, and *in-vitro* release analysis demonstrated a sustained drug-release pattern. High-performance liquid chromatography confirmed the successful loading of esculin and silymarin into the SLNs. The optimized system exhibited improved *in-vitro* cytotoxic effects against HCT-116 colorectal cancer cells compared with the free drugs, although cisplatin showed stronger cytotoxicity than the SLN formulation. Overall, the SLNs displayed favourable physicochemical properties and encouraging *in-vitro* anticancer activity, supporting their potential for future *in-vivo* evaluation.

INTRODUCTION: Cancer is a disease characterized by abnormal cell growth and uncontrolled multiplication anywhere in the body. More than 200 distinct forms of cancer exist. The size, location, stage, and forms of cancer all affect the symptoms and indicators of the disease [1]. Globally, colon cancer ranks third among women and fourth among men. There have been notable differences in colorectal cancer distribution across different countries.

QUICK RESPONSE CODE

DOI: 10.13040/IJPSR.0975-8232.17(5).1657-68

This article can be accessed online on www.ijpsr.com

DOI link: https://doi.org/10.13040/IJPSR.0975-8232.17(5).1657-68

In recently industrialised nations across the world, increasing incidence of colorectal cancer have been documented, even though the risk was previously low [2]. An estimated 136830 new cases of colorectal cancer (CRC) and 50310 patient deaths were reported in the US in 2014. The prevalence of colorectal cancer (CRC) is rising quickly in a number of formerly low-risk regions, such as Spain and several Eastern European and Eastern Asian nations.

More than 170000 new cases of CRC are diagnosed annually in China, where the number of cases and mortality are also rising [3]. 53,200 colorectal cancer-related fatalities and an estimated 104,610 occurrences of colon cancer are anticipated in 2020 [4]. Epidemiologic, clinical, pathologic, and molecular genetic evidence indicate that adenomas

(the adenoma-to-carcinoma sequence) are the primary cause of most colon malignancies [5]. The existing treatments for CRC are insufficient to control metastatic forms of the illness, despite recent advances in our understanding of it. The primary treatment for people with possibly curable colorectal cancer (CRC) is surgery; however, depending on the disease stage, neoadjuvant Echemotherapy or radiotherapy may be administered before or after surgery [6].

However, it is well documented that colorectal cancer (CRC) also impacts the younger population, which has garnered considerable attention in medical research [7]. According to an epidemiological study, up to 40% of colitis patients also had CRC related to their colitis. Through the production of proinflammatory cytokines, the diversification of reactive oxygen species, and the release of nerve signals, inflammatory cells in colonic carcinogenesis contribute to colitis. Oxidative stress may have an impact on a wide range of carcinogenic pathways, as a result of their involvement in increased malignant transformation and started cell proliferation through targets such as DNA, RNA, lipids, and proteins. Because inflammation fosters an inflammatory milieu during the growth of tumour tissue, inflammation also aids in the development of cancer. These cells release inflammatory and immunosuppressive cytokines and chemokines that not only encourage angiogenesis, invasion, metastasis, and proliferation but also weaken the host's immune system and aid in the formation and development of tumours in colorectal cancer [8].

Natural phytoconstituents inhibit cancer-related pathways, such as cellular division, proliferation, angiogenesis, apoptosis, and metastasis [9]. Silymarin, which is derived from the species Silybum marianum, often known as milk thistle, contains a family of closely related flavonolignan chemicals, including silybin. Both *in-vitro* and *in - vivo*, silymarin's chemo preventive action has demonstrated modest efficacy against cancer. silymarin and silybin, its main component, have chemoprotective properties, it is possible to use them to lessen the negative effects and boost the anti-tumour effects of radiation and chemotherapy for a variety of cancer types [10]. Numerous research investigations have suggested that silymarin may inhibit the growth of various tumour cells, including those found in the bladder, colon, ovary, prostate, and breast [11]. Nanoparticles can enhance the medicinal action and drug release of the herbal medication silymarin. The system in nanoparticles is especially helpful for poorly soluble chemicals since it can improve surface area and dissolving rate [12]. Esculin, a glucoside of coumarin, is a prominent active compound found in Cortex fraxini, which is widely utilized in traditional herbal medicine across Asian regions [13].

The structural diversity of coumarins stems from the different types of substitutions on their fundamental rings, which can impact their biological properties [14]. A vast range of phenolic compounds with diverse biological properties, including anti-inflammatory, anti oxidant, anti-mutagenic, and anti-cancer properties, make up coumarins. Furthermore, this is made feasible by the alteration to the coumarin's fundamental ring structure [15]. Solid lipid nanoparticles (SLNs) are a type of colloidal carrier system that have an aqueous surfactant coating encircling a solid core composed of a lipid with a high melting point. Typically, these nanoparticles are used for medications that fall into classes II and IV of the Biopharmaceutics Classification System (BCS). Solid lipid has been long known to be employed as a matrix material for drug delivery, especially when it comes to lipid pellets for oral medication administration [16].

Lipid molecules, which are solid at room temperature, are used to create SLNs. They combine the benefits of a number of different cutting-edge carrier systems, including great biocompatibility, controlled drug release, and physical stability. Moreover, SLN solves a few issues with alternative carrier systems, such as little drug leakage, strong membrane stability, and the viability of large-scale production [17]. The primary concept driving the use of nanoparticle strategies is their capability to efficiently enter tumours passively through the enhanced permeability and retention (EPR) effect. This effect is predominantly a result of the tumour’s leaky vasculature and compromised lymphatic drainage [18]. The most significant advantage of SLN is that the lipid matrix is composed of physiological lipids, lowering the risk of both acute and long-term

toxicity [19]. In the mid-1990s, SLN was unveiled as a novel drug carrier system for oral administration. It has been observed that the adhesive qualities of nanoparticles enhance bioavailability and eliminate irregular oral absorption [20]. Esculin and silymarin are known to exert anticancer effects through partly overlapping mechanisms, such as reducing oxidative stress, promoting apoptosis, and regulating pro-inflammatory and proliferative signalling pathways. Despite these benefits, their clinical utility is constrained by poor water solubility, limited oral bioavailability, and instability under physiological conditions, which can hinder cellular uptake and intracellular delivery. To address these limitations, both compounds were co-encapsulated in a single SLN system as a strategic delivery approach aimed at enhancing physicochemical stability, enabling concurrent transport to the target site, and promoting lipid assisted cellular uptake. This combined delivery strategy may yield additive or potentially synergistic effects while reducing the requirement for higher individual doses, thereby offering a more efficient platform for assessing their *in-vitro* anticancer activity. In order to enable the simultaneous quantification of esculin and silymarin that are loaded into the solid lipid nanoparticles a reverse phase-high performance liquid chromatography (RP-HPLC) method is developed.

MATERIALS AND METHODS:

Materials used: Esculin was purchased from Research Lab Fine Chem Industries in Mumbai, India. Silymarin was obtained from Yucca Enterprises, Mumbai, India. GMS was procured from Loba chemicals, Pvt. Ltd., Mumbai, India. Tween 80 was obtained from Sigma-Aldrich in India. We procured 85% laboratory-grade orthophosphoric acid from S.D. Fine Chem Limited in Mumbai. Merck Mumbai Pvt. Ltd. provided the HPLC grade acetonitrile.

Compatibility Studies (DSC & FTIR)

DSC: To assess the compatibility of esculin and silymarin and to investigate the potential interactions between these compounds, Differential Scanning Calorimetry (DSC) was performed. DSC analysis was performed on GMS, SLY, ESC, Tween 80, and esculin and silymarin loaded SLN. Samples weighing 5 mg each of the mentioned materials were placed in aluminium pans and sealed. The sealed samples were then maintained under isothermal conditions at 20°C for 30 minutes to reach equilibrium. Subsequently, thermograms were recorded by heating the samples from 20°C to 400°C at a rate of 20°C per minute under an inert gas atmosphere [21].

FTIR: FTIR is performed to determine the interactions between drug and excipients The FTIR spectra of esculin and silymarin loaded solid lipid nanoparticles (SLNs), GMS, Tween 80, SLY and ESC in a 1:1 ratio was recorded. The experiment was conducted using a Shimadzu IR instrument. The samples were prepared using the potassium bromide (KBr) pellet method, where each sample was mixed with KBr and compressed into a pellet for subsequent FTIR analysis [22].

Preparation of Esculin and Silymarin Loaded Solid Lipid Nanoparticles: The technique of hot homogenization was utilised to produce solid lipid nanoparticles (SLNs) loaded with silymarin and esculin. The lipid component containing silymarin and esculin was heated to 80°C melting point in a glass container submerged in a hot water bath. Then the emulsifying agent (tween 80) was dissolved in distilled water to create an aqueous phase, which was then heated to the same temperature (80°C) as the oil phase. The melted lipid phase was combined with a hot aqueous phase, which was then homogenised immediately using a T25 digital Ultra Turax IKA homogenizer at 2500 rpm for 10 minutes. Using Ultrasonic Probe sonicator VC750, USA, the dispersion was sonicated for 10 min. The dispersion was then filtered through 0.45 µm filter. It was kept in dark medication bottles at -4°C [23, 24]. Different formulations of solid lipid nanoparticles loaded with esculin and silymarin were carefully prepared, and their specific compositions are detailed in **Table 1.**

TABLE 1: DOE RUNS AND EXPERIMENTAL RESPONSES

Formulation Code	X1	X2	Y1	Y2	Y3
	(%w/w)	(%w/w)	(nm)	(mV)	(%)

F1	5	1.5	244	-48	89.26%
F2	3	1.5	259	-41	86.2%
F3	1	1.5	190	-6.51	86.6%
F4	5	2	174	-45	82.36%
F5	3	2	217	-41	78.4%
F6	1	2	153	-27	84.6%
F7	5	2.5	164	-40.1	77.85%
F8	3	2.5	176	-39	76.8%

X1= GMS, X2= Tween 80, Y1= Particle size, Y2= Zeta potential, Y3= Entrapment Efficiency:

Design of Experiments (DoE): An important aspect of QbD is the design of experiments (DoE), which is used to assess how many critical process parameters (CPP) have an impact on the product's critical quality attributes (CQA). DoE assists in developing high-quality products by reducing the need for conducting a large number of costly and time-consuming experiments [25]. Here, a 2-factor, 3-level factorial experimental design approach was applied to optimize the formulation of solid lipid nanoparticles (SLNs) loaded with esculin and silymarin [26]. As shown in the **Table 2**, tween 80 and GMS served as independent variables. Particle size, zeta potential and %EE were chosen as dependent variables. The response values obtained for all nine factorial batches were analysed using Design Expert software (Stat-Ease, Inc., version 13.0). Statistical analysis of the formulations was conducted using Design-Expert software. To further explore the optimal formulations, nine batches were prepared based on the suggestions provided by the software, employing a surface response factorial design with three levels, two factors, and two responses [27].

Statistical Optimization: The experiments in this study were performed three times (triplicate) to ensure reliability, and the results were presented as the mean values along with the standard deviations. Statistical analysis was carried out using both ANOVA and Student's t-test to assess the significance of the findings, with a significance threshold set at $p < 0.05$.

TABLE 2: SLN FORMULATIONS PREPARED USING A 3^2 FACTORIAL DESIGN

Independent variables	Levels		
	Low (-1)	Medium (0)	High (+1)
X1-GMS	1	3	5
X2-Tween 80	1.5	2	25
Dependent variables	Desired outcomes		
Y1=Particle size	Minimum	+++	
Y2-Zeta potential	In Range	+++	
Y3-Entrapment Efficiency	Maximum	+++	

Evaluation of Esculin and Silymarin Loaded Solid Lipid Nanoparticles:

Particle Size Analysis, PDI: The particle size distribution, including the mean diameter and polydispersity index, was analyzed using with a Malvern Instrument, U.K. The average particle size and polydispersity index were computed for each sample. The dispersion medium used was distilled water, and the measurements were conducted at a constant temperature of 25°C with a measurement position set at 4.65 mm within the system [28].

Zeta Potential: The zeta potential was determined using a Malvern Zeta Sizer Instrument, UK. For this analysis, SLN samples were diluted with double distilled water and introduced into the electrophoretic cell within a cuvette. Each sample was measured three times to ensure accuracy and consistency [29].

Entrapment Efficiency: The percentage of drug entrapped was assessed using a centrifugation method. The nanoparticle dispersion was spun in a centrifuge at 10,000rpm for 20 min. After centrifugation, 0.1mL of the supernatant was extracted and mixed with methanol to make a final volume of 10mL. This diluted solution was subsequently analysed using a UV spectrophotometer at the wavelength of maximum absorption of 311 nm.

The percentage encapsulation efficiency (%EE) was determined using a specific equation based on the obtained data [30].

$$\%EE = W_{total\ drug} - W_{free\ drug} / W_{total\ drug} \times 100$$

$W_{total\ drug}$ = The total amount of drug $W_{free\ drug}$ = The amount of drug into the supernatant.

***In-vitro* Drug Release:** The *in-vitro* release behaviour of silymarin- and esculin-loaded SLNs was assessed using the dialysis membrane diffusion method. A dialysis membrane with a molecular weight cut-off of 12,000–14,000 Da (Sigma) was employed. A 5 mL aliquot of the SLN dispersion was transferred into the membrane, tightly sealed at both ends, and suspended in 900 mL of phosphate buffer (pH 7.4) maintained at 37 ± 2 °C with continuous stirring at 100 rpm. At predetermined time intervals, 3 mL samples were withdrawn from the release medium and replaced with an equal volume of fresh buffer to preserve sink conditions. The withdrawn samples were analyzed spectrophotometrically at 311 nm to quantify the amount of drug released [31].

TEM Analysis: The structure of the SLNs loaded with esculin and silymarin was examined using 200 kV transmission electron microscopy. A single drop of the freshly prepared esculin and silymarin loaded SLNs suspension was put on a copper grid covered in nitrocellulose after being diluted ten times with distilled water. Prior to observation, every sample was air-dried and negatively stained with 2% (w/v) phosphotungstic acid [32].

***In-vitro* Cell Line Study:** The HCT-116 cell line, originating from human colorectal carcinoma, was obtained from the National Centre for cell science (NCCS), Pune, India, for this research study. Following the acquisition of the cell lines, the cells were maintained and sub-cultured by preparing 100 ml of complete media, which consisted of 89 ml of McCoy's 5A supplemented with 10ml Fetal bovine serum (FBS) and 1ml antibiotics. The cells were cultured in a CO2 incubator with 5% carbon dioxide. MTT assay was conducted with cisplatin included as the positive control in the experimental design. Serial dilutions ranging from 100 to 1200 µg/mL were prepared for both the test compound and cisplatin during the experiment. A trypan blue assay was conducted to assess cell viability, and the count of viable cells was determined and quantified. Cells were seeded at a density of $5*10^3$ cells per well in a 96-well plate, followed by the addition of complete media to achieve a final volume of 150 microliters per well. Following 24 hours of incubation in a 5% carbon dioxide environment, once the cells became attached and entered the logarithmic growth phase, the test compound was introduced. The serially diluted compounds were added to the wells and incubated for 24 hours. The supernatant from all the wells was removed, and fresh media was added for further incubation for an additional 24 hours. At the conclusion of the incubation period, a mixture of 20 µl of MTT dye in media was added to each well. The plate was then covered with aluminium foil to protect the MTT dye from light sensitivity and incubated for four hours. The supernatant was carefully aspirated and discarded without disrupting the formazan crystals. Subsequently, 100 ml of dimethyl sulfoxide (DMSO) were added to dissolve the crystals, and the absorbance was measured using a spectrophotometer at approximately 570 nm to obtain readings [33, 34].

Reversed-phase-High Performance Chromatography (RP-HPLC):

Chromatography Conditions: Quantitative estimation of silymarin and esculin in the optimized SLN formulation was performed using an Agilent 1220 Infinity II HPLC system equipped with a PDA detector (SPD-M20A), auto sampler (SIL-20ACHT), binary pump (LC 20AD) with in-line degasser (DGU-20A5), and column oven (CTO-10AS). Separation was achieved on a Phenomenex Luna C18 column (250 × 4.6 mm, 5 µm). A 10 µL aliquot of each sample was injected, and the analysis was conducted at 35 °C with a flow rate of 1.0 mL/min. The mobile phase consisted of acetonitrile and 0.1% orthophosphoric acid in water, ensuring pH stability and efficient resolution of both analytes. Detection was carried out at 311 nm using the PDA detector.

Method Validation: In order to evaluate the method's performance in relation to important parameters including linearity, accuracy, precision, robustness, and the limits of detection (LOD) and quantification (LOQ), the method was validated. To determine the method's linearity, five dilutions were produced from standard stock solutions

ranging from 2-10 µg/ml [35, 36]. The accuracy was determined by analysing the test outcomes to find the percentage of the substance detected by the assay. These assessments followed the standard addition technique at concentrations of 80%, 100%, and 120%, as outlined in the ICH Guideline [37]. The precision of this method was established by injecting multiple injections of the 10 µg/mL solutions of silymarin and esculin, respectively, and determining the root mean square deviation. By assessing the solution on the same day (intra-day precision) and on three distinct days (inter-day), the method's variability was analysed [38]. The robustness of the established method was explored by assessing the impact of minor intentional alterations in procedural factors such as change in flow rate and wavelength [39]. The developed method's limit of detection (LOD) and limit of quantification (LOQ) were estimated using the ICH guideline formula [40].

RESULTS AND DISCUSSION

Compatibility Studies (DSC & FTIR):

DSC: Differential Scanning Calorimetry (DSC) was performed to examine potential interactions between the drugs and the excipients. **Fig. 1** shows the DSC thermograms of the pure drugs, glyceryl monostearate (GMS), surfactant, physical mixture, and the SLN formulation. The distinct endothermic melting peak of GMS seen in its pure form was also present in the physical mixture, indicating that the lipid maintained its crystalline structure. Although, the SLN formulation exhibited disappearance or broadening of the characteristic drug melting peaks, indicating decreased crystallinity or molecularly dispersed form within the lipid matrix. These observations suggest no major drug–excipient incompatibility and supports successful incorporation of the drugs into the SLN system.

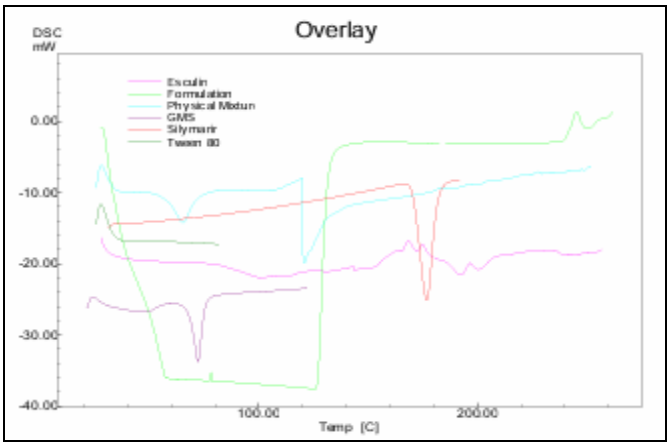

FIG. 1: DSC THERMOGRAMS OF DRUG, EXCIPIENTS, PHYSICAL MIXTURE, AND SLN FORMULATION

FTIR: Esculin and silymarin underwent Fourier transform infrared (FTIR) analysis, which revealed the presence of numerous distinguishable functional groups. **Fig. 2** shows the persistence of recognisable peaks in the drug and excipient mixture indicates compatibility between the components. This observation confirms that the distinct chemical identities of both the medication and the excipients remain stable in the composite system.

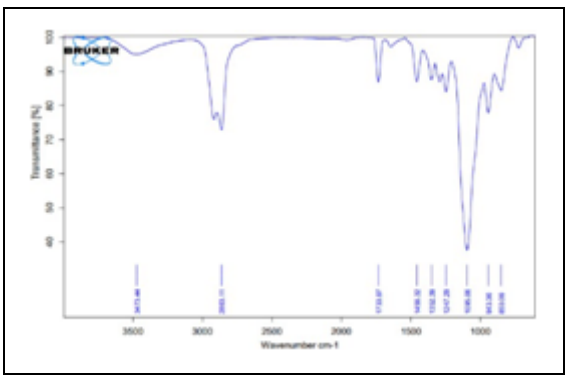

FIG. 2: FTIR SPECTRUM OF PHYSICAL MIXTURE (ESCULIN, SILYMARIN, GMS, TWEEN 80)

Optimization of Esculin and Silymarin Loaded Solid Lipid Nanoparticles by DoE Approach: A study used a 32 factorial design with a total of 9 trials to investigate the effects of two factors. This design consists of 2 factors and 3 levels. Graphical presentation of particle size is given in **Fig. 3**. The equation of Particle size (Y1), PS = +208.44+ $17.33 * A - 36.33 * B - 6.25 * AB - 40.67 * A2 + 13.33 *$ shows that coefficient of A is positive, indicating an increase in particle size to the optimum level. The coefficient of B is negative, indicating a decrease in particle size (Y1).

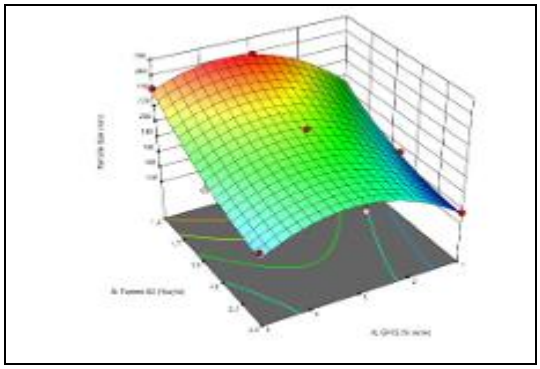

FIG. 3: RESPONSE SURFACE PLOT FOR RESPONSE Y1 (PARTICLE SIZE)

Fig. 4 reveals the graphical presentation of zeta potential. The equation of zeta potential (Y2), $ZP = -35.52 - 11.28 * A - 2.61 * B + 8.33 * AB$ shows gradual decrease in A's coefficient because it is displaying a negative sign. Similar to A, B's coefficient also has a negative sign, which causes the zeta potential to drop.

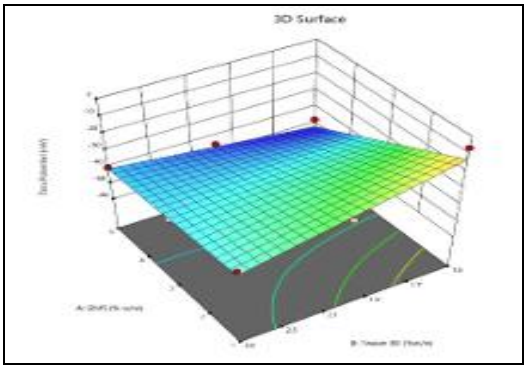

FIG. 4: RESPONSE SURFACE PLOT FOR RESPONSE Y2 (ZETA POTENTIAL)

Graphical presentation of entrapment efficiency is disclosed in **Fig. 5**. The equation of entrapment efficiency (Y3), $EE = +79.78 - 0.3217 * A - 4.54 * B - 1.25 * AB + 3.01 * A2 + 1.03 * B2$ shows the coefficient of A as well as B indicates the negative sign which shows decrease in B entrapment efficiency.

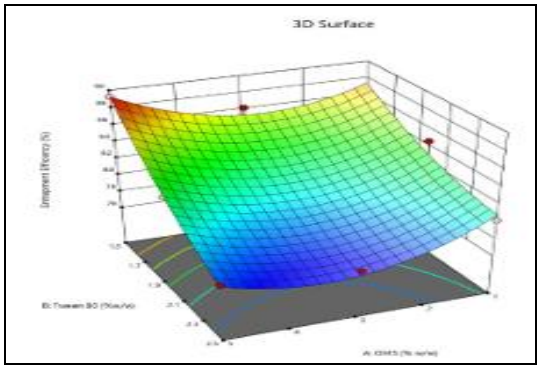

FIG. 5: RESPONSE SURFACE PLOT FOR RESPONSE Y3 (ENTRAPMENT EFFICIENCY)

Statistical Optimization: The lack-of-fit test was found to be non-significant for all responses ($p > 0.05$), indicating that the model provided a suitable fit to the experimental data. In addition, Adeq Precision values exceeding for each response demonstrated an adequate signal-to-noise ratio, confirming the robustness of the model. Results from Student's t-test further verified that the main and interaction effects of GMS and Tween-80 concentrations on the evaluated responses were statistically significant ($p < 0.05$). Taken together, these outcomes confirm that the selected quadratic model is appropriate and statistically reliable for optimizing the SLN formulation. **Table 3** represents the statistical parameters.

TABLE 3: MODEL STATISTICS FOR DOE RESPONSES

Response	R2	Predicted R^2	Adjusted R^2	p-value	F-value
Particle Size (Y1)	0.9724	0.7193	0.9263	0.0152	21.11
Zeta Potential (Y2)	0.8622	0.2574	0.7795	0.0136	10.43
Entrapment Efficiency (Y3)	0.9600	0.6421	0.8934	0.0262	14.40

Evaluation of Esculin and Silymarin Loaded Solid Lipid Nanoparticles

Particle Size Analysis, PDI: The homogenization technique yielded solid lipid nanoparticles with mean particle sizes ranging from 135 to 259 nm. The polydispersity index (PDI) values varied between 0.2831 and 0.8294 across the batches, indicating that some of the preliminary formulations exhibited a broad particle size distribution and partial polydispersity. However, the optimized formulation (F6) demonstrated a lower PDI reflecting a more uniform nanoparticle population and better formulation stability.

Zeta Potential: The zeta potential of the SLN formulations ranged from −6.51 mV to −48 mV, with the negative charge attributed to free fatty acids in glycerol monostearate. Formulations with higher negative values (−25 mV to −48 mV) are expected to possess stronger electrostatic stability, whereas those with lower absolute values (−6.51 mV to −15 mV) may be more susceptible to aggregation. This suggests that such batches may depend primarily on steric stabilization provided by Tween-80, and their long term stability requires further verification.

Entrapment Efficiency: The percentage of free and total drug in the SLN formulations was assessed, and the optimized batch demonstrated an entrapment efficiency (EE) of 84.6%. The relatively high EE may be partly attributed to the use of an appropriate surfactant concentration, which supports drug solubilization within the lipid matrix. Nonetheless, EE is also influenced by other factors such as lipid composition, drug–lipid interactions, and processing parameters. Accordingly, surfactant concentration should be regarded as one contributing factor rather than the sole determinant of the observed EE.

***In-vitro* Drug Release:** The *in-vitro* release behaviour of the optimized SLN formulation **Fig. 6** was assessed in pH 7.4 buffer using a dissolution apparatus equipped with a small-volume adapter. The formulation demonstrated a biphasic release pattern, with cumulative releases of 84.28% for esculin and 63.98% for silymarin at 24 hours. Analysis of the release data indicated that the zero-order kinetic model provided the best fit, with R^2 values of 0.9794 for both drugs **Fig. 7.**

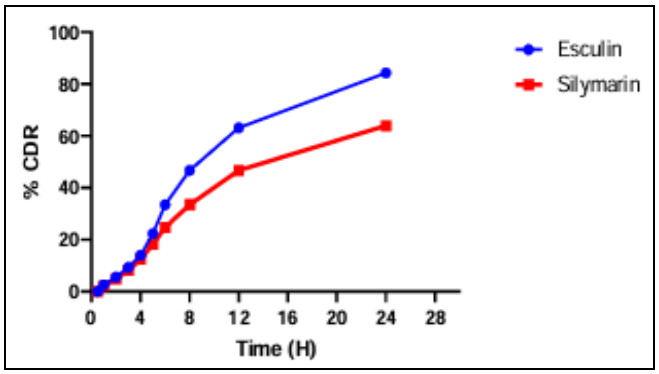

FIG. 6: *IN-VITRO* DRUG RELEASE OF SOLID LIPID NANOPARTICLES

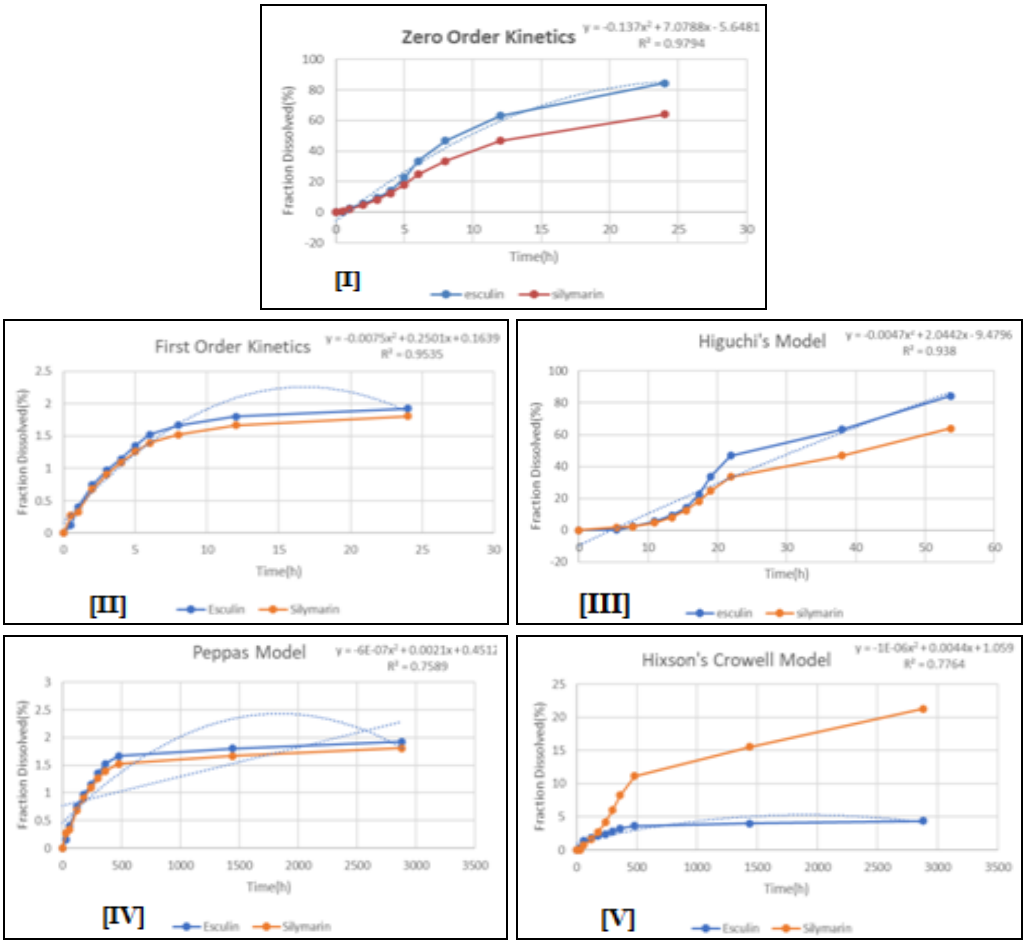

FIG. 7: (I, II, III, IV, V) KINETIC ANALYSIS OF DRUG RELEASE OF SOLID LIPID NANOPARTICLES

TEM Analysis: The morphology of the solid lipid nanoparticles was evaluated using transmission electron microscopy (TEM). The images revealed that the nanoparticles exhibited a predominantly spherical shape with smooth, well-defined surfaces, reflecting good structural integrity. The particle cores visualized under TEM were observed in the range of 100–500 nm **Fig. 8**; however, these measurements correspond to the dehydrated solid cores imaged under vacuum conditions.

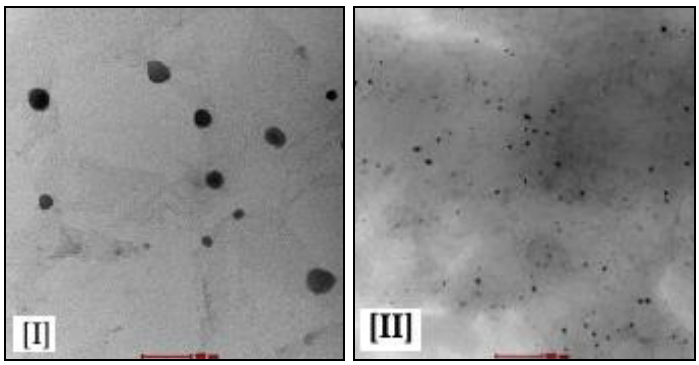

FIG. 8: [I, II] TEM IMAGE OF OPTIMIZED SOLID LIPID NANOPARTICLES

In-vitro Cell line study The MTT assay confirmed that the SLN formulation exerted notable cytotoxic effects against HCT-116 cells. After 24 hours, the SLNs produced 47.1% cell viability at a concentration of 1200 µg/mL, whereas the positive control, cisplatin (1 µg/mL), yielded a viability of 17.6% **Fig. 9**. The IC_{50} value of the SLN formulation against HCT-116 cells was determined to be approximately 1040 µg/mL at 24 hours, based on dose–response curve interpolation. Overall, the results indicate that the SLN system improves the in-vitro anticancer performance of esculin and

silymarin compared with the free drug, although its cytotoxicity remains lower than that of cisplatin.

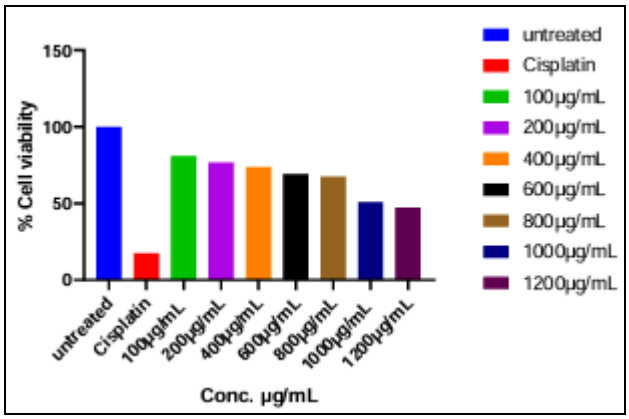

FIG. 9: BAR GRAPH OF HCT-116 CELL VIABILITY

Reverse-phase High Performance Liquid Chromatography (RP-HPLC): The optimized HPLC method enabled accurate and reliable quantification of esculin and silymarin in the SLN formulation, yielding well-resolved peaks at retention times of 3.004 and 10.986 minutes, respectively. The reproducibility of these retention times confirms the robustness of the chromatographic method **Fig. 10** and **11.** Method validation conducted in accordance with ICH Q2(R1) showed that all analytical parameters were within acceptable limits, as presented in **Table 4.** Although the recovery of silymarin at the 150% level was slightly lower (97.01%) than the values obtained at other levels, it remains within the acceptable recovery range (95–105%), indicating no significant loss or matrix interference at higher concentrations.

TABLE 4: VALIDATION PARAMETERS OF HPLC METHOD DEVELOPMENT

Sr. no.	Validation parameters	Esculin	Silymarin
1	**Linearity**		
	Linearity range (µg/mL)	2-10	2-10
	Correlation-coefficient	0.9974	0.9991
2	LOD (µg/mL)	0.30	0.61
	LOQ (µg/mL)	0.92	1.85
3	**Precision**		
	Intra-day (%RSD)	0.51	0.36
	Inter-day (%RSD)	1.24	0.32
4	**Robustness**		
	Change in Mobile phase volume (%RSD)	0.72	0.75
	Change in flow rate (%RSD)	0.21	0.85
5	**Accuracy**		
	50% recovery	98.01±0.03	101.03±0.27
	100% recovery	100.14±0.85	100.81±0.56
	150% recovery	98.41±0.54	97.01±0.21

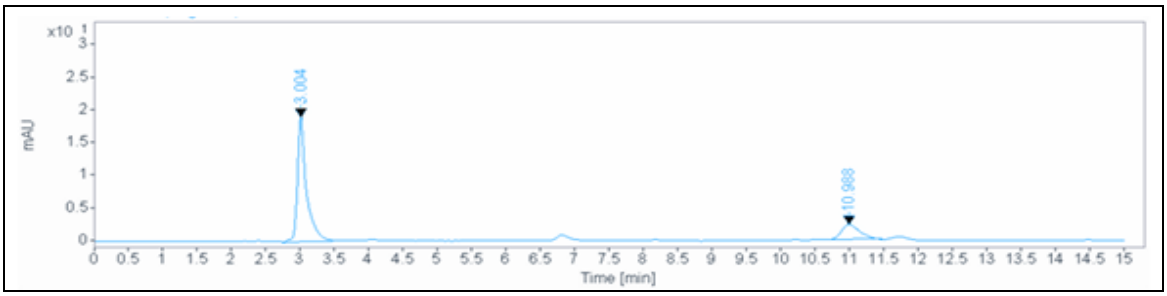

FIG. 10: HPLC CHROMATOGRAM OF ESCULIN AND SILYMARIN

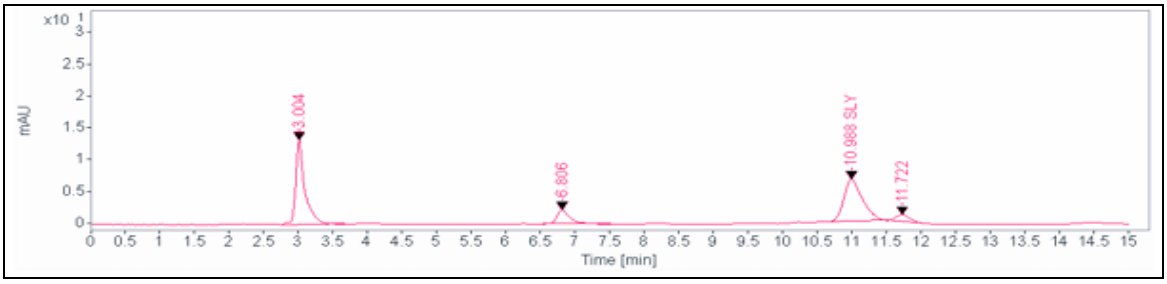

FIG. 11: HPLC CHROMATOGRAM OF SOLID LIPID NANOPARTICLES

CONCLUSION: The study successfully formulated and optimized solid lipid nanoparticles loaded with esculin and silymarin using a Design-Expert–assisted factorial design approach. The optimized batch (F6), prepared with 1% GMS and 2% Tween-80, demonstrated favorable physicochemical attributes, including a nanoscale particle size of 153 nm, a zeta potential of −27 mV, and an entrapment efficiency of 84.6%. A simultaneous HPLC analytical method was also developed and validated for both drugs within the formulation, yielding distinct and well resolved retention peaks. *In-vitro* cytotoxic evaluation against the HCT-116 colorectal cancer cell line revealed a concentration dependent decrease in cell viability for the SLN formulation, although its activity remained lower than that of cisplatin. These findings suggest enhanced In-vitro performance of the developed SLNs relative to the free drug; however, the outcomes are confined to laboratory-scale experimentation.

ACKNOWLEDGEMENT: Authors are grateful to Department of pharmaceutical Quality Assurance, Department of pharmaceutics and KLE College of Pharmacy, Belagavi, for providing necessary facilities.

CONFLICT OF INTEREST: The authors declare no conflict of interest.

REFERENCES:

1. George BP, Chandran R and Abrahamse H: Role of phytochemicals in cancer chemoprevention: insights. Antioxidants 2021; 10(9): 1455.
2. Center MM, Jemal A, Smith RA and Ward E: Worldwide variations in colorectal cancer. CA Cancer J Clinicians 2009; 59(6): 366-78.
3. Li YH, Niu YB, Sun Y, Zhang F, Liu CX, Fan L and Mei QB: Role of phytochemicals in colorectal cancer prevention. World J Gastroenterology 2015; 21(31): 9262.
4. Zhu X, Parks PD, Weiser E, Fischer K, Griffin JM, Limburg PJ and Rutten LJF: National survey of patient factors associated with colorectal cancer screening preferences. Cancer Prev Res 2021; 14(5): 603-14.
5. Cappell MS: Pathophysiology, clinical presentation and management of colon cancer. Gastroenterol Clin North Am 2008; 37(1): 1-24.
6. Redondo-Blanco S, Fernández J, Gutiérrez-del- Río I, Villar CJ and Lombó F: New insights toward colorectal cancer chemotherapy using natural bioactive compounds. Front Pharmacology 2017; 8: 242711.
7. O'Connell JB, Maggard MA, Livingston EH and Clifford KY: Colorectal cancer in the young. Am J Surgery 2004; 187(3): 343-8.
8. Pan MH, Lai CS, Wu JC and Ho CT: Molecular mechanisms for chemoprevention of colorectal cancer by natural dietary compounds. Mol Nutr Food Res 2011; 55(1): 32-45.
9. Ranjan A, Ramachandran S, Gupta N, Kaushik I, Wright S and Srivastava S: Role of phytochemicals in cancer prevention. Int J Mol Sci 2019; 20(20): 4981.
10. Emadi SA, Rahbardar MG, Mehri S and Hosseinzadeh H: Therapeutic potentials of milk thistle (*Silybum marianum* L.) and silymarin on cancer: a review. Iran J Basic Med Sci 2022; 25(10): 1166-76.
11. Fallah M, Davoodvandi A, Nikmanzar S, Aghili S, Mirazimi SM and Aschner M: Silymarin as a therapeutic agent in gastrointestinal cancer. Biomed Pharmacotherapy 2021; 142: 112024.
12. Ubaidulla U, Sinha P, Sangavi T and Rathnam G: Development of silymarin- entrapped chitosan phthalate nanoparticles for targeting colon cancer. J Nat Remedies 2022; 22: 659-71.
13. Rehman SU, Kim IS, Kang KS and Yoo HH: HPLC determination of esculin and esculetininrat plasma for pharmacokinetic studies. J Chromatographic Sci 2015; 53(8): 1322-7.
14. Kang KS, Lee W, Jung Y, Lee JH, Lee S and Eom DW: Protective effect of esculin on streptozotocin-induced diabetic renal damage in mice. J Agric Food Chem 2014; 62(9): 2069-76.
15. Patil S, Adhyapak A, Shetti P and Gurao R: RP-HPLC method development for determination of esculin using AQbD principles. Future J Pharm Sci 2023; 9(1): 69.
16. Lingayat VJ, Zarekar NS and Shendge RS: Solidlipid nanoparticles: a review. Nanosci Nanotechnol Res 2017; 4(2): 67-72.
17. Rajpoot K and Jain SK: Colorectal cancer- targeted delivery of oxaliplatin via folic acid-grafted solid lipid nanoparticles. Artificial Cells Nanomedicine & Biotechnology 2018; 46(6): 1236-47.
18. Tummala S, Kumar MS, Gowthamarajan K, Prakash A, Raju KR and Mulukutla S: Oxaliplatin solid lipid nanoparticles for colorectal cancer: preparation and evaluation. Indo Am J Pharm Res 2014; 4: 3579-87.
19. Mehnert W and Mäder K: Solid lipid nanoparticles: production, characterization and applications. Adv Drug Deliv Rev 2012; 64: 83-101.
20. Üner M and Yener G: Importance of solid lipid nanoparticles in various administration routes. Int J Nanomed 2007; 2(3): 289-300.
21. Patel D, Patel M, Soni T and Suhagia B: Topical arginine solid lipid nanoparticles: QbD-based development and characterization. J Drug Deliv Sci Technol 2021; 61: 102329.
22. Nair R, Priya KV, Kumar KA, Badivaddin TM and Sevukarajan M: Formulation and evaluation of solid lipid nanoparticles of isoniazid. J Pharm Sci Res 2011; 3(5): 1256-60.
23. Bhalekar MR, Pokharkar V, Madgulkar A and Patil N: Miconazolenit rate-loaded solid lipid nanoparticles for topical delivery. AAPS Pharm Sci Tech 2009; 10: 289-96.
24. Al-Haj NA: Tamoxifen-loaded solid lipid nanoparticles prepared by hot high-pressure homogenization. Am J Pharmacol Toxicol 2008; 3(3): 219-24.
25. Shah B, Khunt D, Bhatt H, Misra M and Padh H: QbD-based intranasal delivery of rivastigmine-loaded solid lipid nanoparticles. Eur J Pharm Sci 2015; 78: 54-66.
26. Pardeshi CV, Rajput PV, Belgamwar VS, Tekade AR and Surana SJ: Surface- modified solid lipid nanoparticles for intranasal delivery of ropinirole. Drug Deliv 2013; 20(1): 47-56.

27. Sailor GU, Ramani VD, Shah N, Parmar GR, Gohil D, Balaraman R and Seth A: DoE-based optimization of berberine- loaded solid lipid nanoparticles. Indian J Pharm Sci 2021; 83(2): 204-18.
28. Nair R, Kumar AC, Priya VK, Yadav CM and Raju PY: Chitosan solid lipid nanoparticles of carbamazepine. Lipids Health Dis 2012; 11(1): 72.
29. Begum MY and Gudipati PR: Formulation and evaluation of dasatinib-loaded solid lipid nanoparticles. Int J Pharm Pharm Sci 2018; 10: 14-20.
30. Raina H, Kaur S and Jindal AB: Efavirenz- loaded solid lipid nanoparticles: QbD-based optimization and characterization. J Drug Deliv Sci Technol 2017; 39: 180-91.
31. Kumari P, Rachna UK, Ravikant AG and Sagheer R: Silymarin-loaded solid lipid nanoparticles for liver cirrhosis: development and validation. J Pharm Negative Results 2022; 11: 5871-87.
32. JiP, Yu T, Liu Y, Jiang J, Xu J and Zhao Y: Naringenin-loaded solid lipid nanoparticles: preparation and pulmonary pharmacokinetics. Drug Des Devel Ther 2016; 10: 911-25.
33. Sezer CV: An *in-vitro* assessment of the cytotoxic and apoptotic potency of silymarin and silymarin-loaded solid lipid nanoparticles on lung and breast cancer cells. Pak J Zool 2021; 53(4): 1-9.
34. Hogan FS, Krishnegowda NK, Mikhailova M and Kahlenberg MS: Silibinin inhibits proliferation of human colon cancer cells. J Surg Res 2007; 143(1): 58-65.
35. Korany MA, Haggag RS, Ragab MA and Elmallah OA: Stability-indicating HPLC method for simultaneous determination of silymarin and curcumin. Arab J Chem 2017; 10(2): 1711-25.
36. Kharoaf M, Malkieh N, Abualhasan M, Shubitah R, Jaradat N and Zaid AN: Stability-indicating HPLC method for valsartan and hydrochlorothiazide tablets. Int J Pharm Pharm Sci 2012; 4(3): 284-90.
37. Shrikrishna B and Nisharani R: Simultaneous estimation of montelukast and ebastine by HPLC. Res J Pharm Technol 2015; 8(1): 1-5.
38. TD R.P-HPLC. Method development and validation for the simultaneous estimation of ofloxacin and ornidazole in tablet dosage form by RP-HPLC. Methods 2010; 1(1): 78-83.
39. Shah Y, Iqbal Z, Ahmad L, Khan A, Khan MI and Nazir S: Simultaneous determination of rosuvastatin and atorvastatin in human serum by RP-HPLC. J Chromatogr B 2011; 879(9-10): 557-63.
40. Shah P, Pandya T, Gohel M and Thakkar V: HPLC method for simultaneous estimation of rifampicin and ofloxacin using experimental design. J Taibah Univ Sci 2019; 13(1): 146-54

How to cite this article:
Birje K and Shelar O: Designing efficient solid lipid nanoparticles for colorectal cancer: formulation and evaluation of esculin and silymarin using doe approach. Int J Pharm Sci & Res 2026; 17(5): 1657-68. doi: 10.13040/IJPSR.0975-8232.17(5).1657-68.

All © 2026 are reserved by International Journal of Pharmaceutical Sciences and Research. This Journal licensed under a Creative Commons Attribution-NonCommercial-ShareAlike 3.0 Unported License.

This article can be downloaded to **Android OS** based mobile. Scan QR Code using Code/Bar Scanner from your mobile. (Scanners are available on Google Playstore)